nature immunology

The p110δ isoform of the kinase PI(3)K controls the subcellular compartmentalization of TLR4 signaling and protects from endotoxic shock

Ezra Aksoy[1], Salma Taboubi[1], David Torres[2,6], Sandrine Delbauve[2,6], Abderrahman Hachani[3], Maria A Whitehead[1], Wayne P Pearce[1], Inma M Berenjeno[1], Gemma Nock[1], Alain Filloux[3], Rudi Beyaert[4,5], Veronique Flamand[2] & Bart Vanhaesebroeck[1]

© 2012 Nature America, Inc. All rights reserved.

Lipopolysaccharide activates plasma-membrane signaling and endosomal signaling by Toll-like receptor 4 (TLR4) through the TIRAP-MyD88 and TRAM-TRIF adaptor complexes, respectively, but it is unclear how the signaling switch between these cell compartments is coordinated. In dendritic cells, we found that the p110δ isoform of phosphatidylinositol-3-OH kinase (PI(3)K) induced internalization of TLR4 and dissociation of TIRAP from the plasma membrane, followed by calpain-mediated degradation of TIRAP. Accordingly, inactivation of p110δ prolonged TIRAP-mediated signaling from the plasma membrane, which augmented proinflammatory cytokine production while decreasing TRAM-dependent endosomal signaling that generated anti-inflammatory cytokines (interleukin 10 and interferon-β). In line with that altered signaling output, p110δ-deficient mice showed enhanced endotoxin-induced death. Thus, by controlling the 'topology' of TLR4 signaling complexes, p110δ balances overall homeostasis in the TLR4 pathway.

Toll-like receptors (TLRs) are evolutionarily conserved pathogen-recognition molecules expressed by professional antigen-presenting dendritic cells (DCs) and macrophages[1,2]. TLR4 is the best-characterized member of this family; it recognizes lipopolysaccharide (LPS) from the cell walls of Gram-negative bacteria[2]. TLR4 signaling comprises two distinct signaling pathways, referred to as 'MyD88-dependent' and 'MyD88-independent' that both culminate in the expression of genes encoding inflammatory and immunomodulatory molecules[2]. The MyD88-dependent pathway is mediated by the adaptors MyD88 and TIRAP (Mal) and operates at the plasma membrane[3] to induce transcription factor NF-κB and mitogen-activated protein kinase (MAPK) pathways. The MyD88-independent pathway is initiated by the adaptors TRAM and TRIF in the endosomes[4] to generate interferon-β (IFN-β) through activation of the transcription factor IRF3 (ref. 2). It is thought that the TIRAP-MyD88 pathway transits sequentially into TRAM-TRIF signaling, but the molecular mechanism underlying this switch is unknown.

Phosphatidylinositols are anionic membrane lipids that can provide 'sorting codes' for the recruitment of cytosolic proteins with lipid-binding modules to the membrane[5,6]. Phosphatidylinositols are important determinants for the targeting of TIRAP and TRAM to specific cellular locations, where they act as molecular scaffolds to initiate downstream signaling[7]. A polybasic domain in TIRAP is critical for its binding to regions of the plasma membrane rich in phosphatidylinositol-(4,5)-bisphosphate (PtdIns(4,5)P_2)[3]. TRAM contains a polybasic region that can bind any phosphatidylinositol molecule and also has a myristoylation motif[4] that facilitates the trafficking of proteins from the plasma membrane into endosomes[8].

The turnover of phosphatidylinositols is controlled by lipid kinases and phosphatases and regulates the intracellular sorting of proteins[5]. Members of phosphatidylinositol-3-OH kinase (PI(3)K) class I generate the second messenger phosphatidylinositol-(3,4,5)-trisphosphate (PtdIns(3,4,5)P_3), which is important for a broad range of cell responses, including proliferation, cytoskeletal dynamics and vesicular trafficking[9]. Mammals have eight PI(3)K isoforms that are divided into three classes[10]. The class IA PI(3)K catalytic subunits (p110α, p110β and p110δ) are found in complex with the Src-homology 2 domain–containing regulatory subunit p85 and are acutely activated by tyrosine kinases or G protein–coupled receptors. The class IB PI(3)K p110γ is found in complex with a p84 or p101 regulatory subunit that lacks Src-homology 2 domains and couples to G protein–coupled receptors. The PI(3)K family members p110α and p110β are ubiquitous, and whereas inactivation of p110α leads to full embryonic death, inactivation of p110β leads to partial embryonic death[11,12]. Leukocytes show considerable enrichment for p110γ and p110δ, which control immunological functions[13,14]. All p110 isoforms convert

[1]Centre for Cell Signaling, Barts Institute of Cancer, Queen Mary, University of London, London, UK. [2]Institute for Medical Immunology, Free University of Brussels, Gosselies, Belgium. [3]Division of Cell and Molecular Biology, Centre for Molecular Microbiology and Infection, Imperial College London, London, UK. [4]Department for Molecular Biomedical Research, Unit of Molecular Signal Transduction in Inflammation, VIB, Ghent, Belgium. [5]Department of Biomedical Molecular Biology, Ghent University, Ghent, Belgium. [6]These authors contributed equally to this work. Correspondence should be addressed to B.V. (bart.vanh@qmul.ac.uk) or E.A. (e.aksoy@qmul.ac.uk).

Received 11 August; accepted 20 August; published online 30 September 2012; corrected after print 8 April 2013; doi:10.1038/ni.2426

PtdIns(4,5)P_2 to PtdIns(3,4,5)P_3, which interacts with specific pleckstrin homology domains present in several effector proteins, including the serine-threonine kinase Akt (PKB)[10]. The PI(3)K-Akt axis is activated downstream of TLRs[15], but the precise roles and mechanism of action of individual PI(3)K isoforms in the TLR4 pathway remain unknown. It has also remained unclear whether PI(3)K serves a positive or negative role in TLR signaling, with published evidence supporting both possibilities[16–19].

As PtdIns(4,5)P_2-dependent targeting of TIRAP to the plasma membrane is a prerequisite for the initiation of MyD88-dependent signaling[3], here we explored whether acute regulation of the abundance of PtdIns(4,5)P_2 by PI(3)K would influence TLR4 signaling at this location. We used bone marrow–derived DCs (BMDCs) in which class I PI(3)K isoforms were genetically or pharmacologically inactivated. We found that p110δ was the main class I PI(3)K isoform recruited to the activated TLR4 complex, where it converted PtdIns(4,5)P_2 to PtdIns(3,4,5)P_3 after activation by LPS. The change in the ratio of PtdIns(4,5)P_2 to PtdIns(3,4,5)P_3 concurrently 'licensed' the internalization of TLR4 from the plasma membrane and promoted the redistribution of TIRAP to cytoplasmic compartments, where it was degraded by calpain and proteasome action. Interference with the kinase activity of p110δ extended the residence of TIRAP at the plasma membrane, which led to prolonged signaling via NF-κB and the MAPK p38 and amplified production of proinflammatory cytokines. Conversely, IRF3 activation was diminished, which led to lower expression of IFN-β and anti-inflammatory interleukin 10 (IL-10). *In vivo*, altered TLR4 signaling output led to more endotoxin-induced death of p110δ-deficient mice. Our data document a role for the p110δ isoform of PI(3)K in the compartmentalization of signaling downstream of TLR4.

RESULTS

PI(3)K p110δ controls LPS-induced TLR4 internalization in DCs

BMDCs and splenic DCs express all class I PI(3)K isoforms, but the roles of these kinases in TLR4 signaling are unknown. We initially focused on the p110δ isoform, as it has high expression in leukocytes[10]. We made use of p110δ(D910A) mice (called 'δ(D910A) mice' here), in which the kinase activity of endogenous p110δ is rendered inoperative because of an inactivating germline knock-in mutation in the sequence encoding its catalytic domain[14]. This inactivation of p110δ did not affect expression of the nontargeted p110 and p85 isoforms and had no discernable effect on the number of DCs obtained *in vitro* or *in vivo* (**Supplementary Fig. 1a**,**b**). Splenic DCs from wild-type and δ(D910A) mice had similar expression of the surface markers CD11c and CD8 (**Supplementary Fig. 1c**), and BMDCs of both genotypes had similar expression of major histocompatibility complex class II and the costimulatory molecule CD40 before and after stimulation with LPS (**Supplementary Fig. 1d**). The surface expression of TLR4 on BMDCs and splenic DCs from δ(D910A) and wild-type mice was also similar (**Fig. 1a**,**b** and **Supplementary Fig. 1d**).

PtdIns(3,4,5)P_3 has been linked to phagocytosis and endocytosis[20,21]. Inactivation of p110δ did not notably affect the phagocytosis of *Escherichia coli* opsonized by immunoglobulin G or the macropinocytosis of dextran under basal or LPS-activated conditions (**Supplementary Fig. 1e**). In contrast, endocytosis of the transferrin receptor (**Supplementary Fig. 1e**) and LPS-mediated endocytosis of the TLR4 were significantly inhibited in BMDCs and splenic DCs from δ(D910A) mice relative to their endocytosis in cells from wild-type mice (**Fig. 1a**,**b**); however, 24 h after LPS stimulation, cells from neither mouse strain had detectable TLR4 on their cell surface (**Supplementary Fig. 1d**). Our data indicated that internalization of TLR4 involved p110δ kinase activity.

The p85 immunoprecipitates of δ(D910A) BMDC extracts had ~50% as much *in vitro* PI(3)K activity, under basal or LPS-activated conditions, as wild-type cells had, without a change in the activity of p110α or p110β (**Fig. 1c**). Visualization of the abundance of PtdIns(3,4,5)P_3 by confocal microscopy with antibody to PtdIns(3,4,5)P_3 (anti-PtdIns(3,4,5)P_3) in wild-type cells showed a robust LPS-induced PtdIns(3,4,5)P_3 signal at the cell periphery located together with the cortical actin network (**Supplementary Fig. 2**), which reportedly shows enrichment for the PtdIns(4,5)P_2 substrate for PI(3)K[6]. In contrast, we detected only diffuse PtdIns(3,4,5)P_3 staining in LPS-treated δ(D910A) BMDCs (**Supplementary Fig. 2**). Together these data demonstrated that p110δ was the main PI(3)K isoform in BMDCs that generated PtdIns(3,4,5)P_3 after stimulation with LPS.

In line with those findings, inactivation of p110δ, either pharmacologically (with the ATP-competitive kinase inhibitor IC87114) or genetically (in δ(D910A) cells), inhibited PtdIns(3,4,5)P_3-dependent phosphorylation of Akt after LPS stimulation at early time points (15–30 min), with some residual phosphorylation of Akt occurring at a later time point (60 min; **Fig. 1d**). Genetic or pharmacological inactivation of p110α, p110β or p110γ did not affect LPS-stimulated phosphorylation of Akt, nor did combined pharmacological inactivation of these p110 isoforms (**Supplementary Table 1** and data not shown). The pan-PI(3)K inhibitor wortmannin inhibited the phosphorylation of Akt to an extent similar to that achieved by IC87114 after 30 min of stimulation with LPS (data not shown). Together these data showed that p110δ was the main driver of the LPS-induced PI(3)K-Akt pathway in BMDCs, at least during the early phases of TLR4 signaling.

The TLR4 signaling complex includes p110δ

The data reported above indicated involvement of p110δ in the early steps of TLR4 signaling. To gain molecular insight into the signaling affected by inactivation of p110δ, we first assessed the involvement of known TLR4 adaptors in LPS-induced activation of PI(3)K. LPS-induced phosphorylation of Akt was unaffected in TRIF-deficient cells but was absent in TLR4-deficient cells and was much lower in MyD88- or TIRAP-deficient cells (**Fig. 1e**). Immunoprecipitation with anti-TLR4 or anti-p110δ showed that p110δ was recruited to an early LPS-induced signalosome complex that contained TLR4, MyD88 and TIRAP in both wild-type and δ(D910A) BMDCs (**Fig. 1f**,**g**). The p110δ immunoprecipitates also had a weakly detectable enhanced interaction of TRAM with TLR4 that we did not observe in δ(D910A) BMDCs (**Fig. 1g**); this indicated less interaction of TRAM with activated TLR4 in the absence of p110δ kinase activity. Furthermore, LPS-induced interaction of p110δ with MyD88 occurred before the binding of p110δ to TIRAP (**Fig. 1g**). Together these data showed that p110δ was recruited to the newly formed TLR4 complex at an early stage and that TIRAP and MyD88 but not TRIF were essential for LPS-induced activation of the p110δ PI(3)K–Akt axis, with possible involvement of p110δ in promoting the TRAM-TLR4 interaction after stimulation with LPS.

PI(3)K p110δ dissociates TIRAP from the plasma membrane

The stimulation of phospholipases and PI(3)Ks via receptors can modify the local plasma-membrane concentration of PtdIns(4,5)P_2 (refs. 22,23), which is important for the localization of TIRAP to this site[3] and could thus contribute to TLR4 signaling. We therefore investigated whether p110δ activity influenced the localization of TIRAP at the plasma membrane under basal and LPS-stimulated conditions. Under basal conditions, the distribution of endogenous TIRAP was similar in wild-type and δ(D910A) BMDCs, as it localized along the

© 2012 Nature America, Inc. All rights reserved.

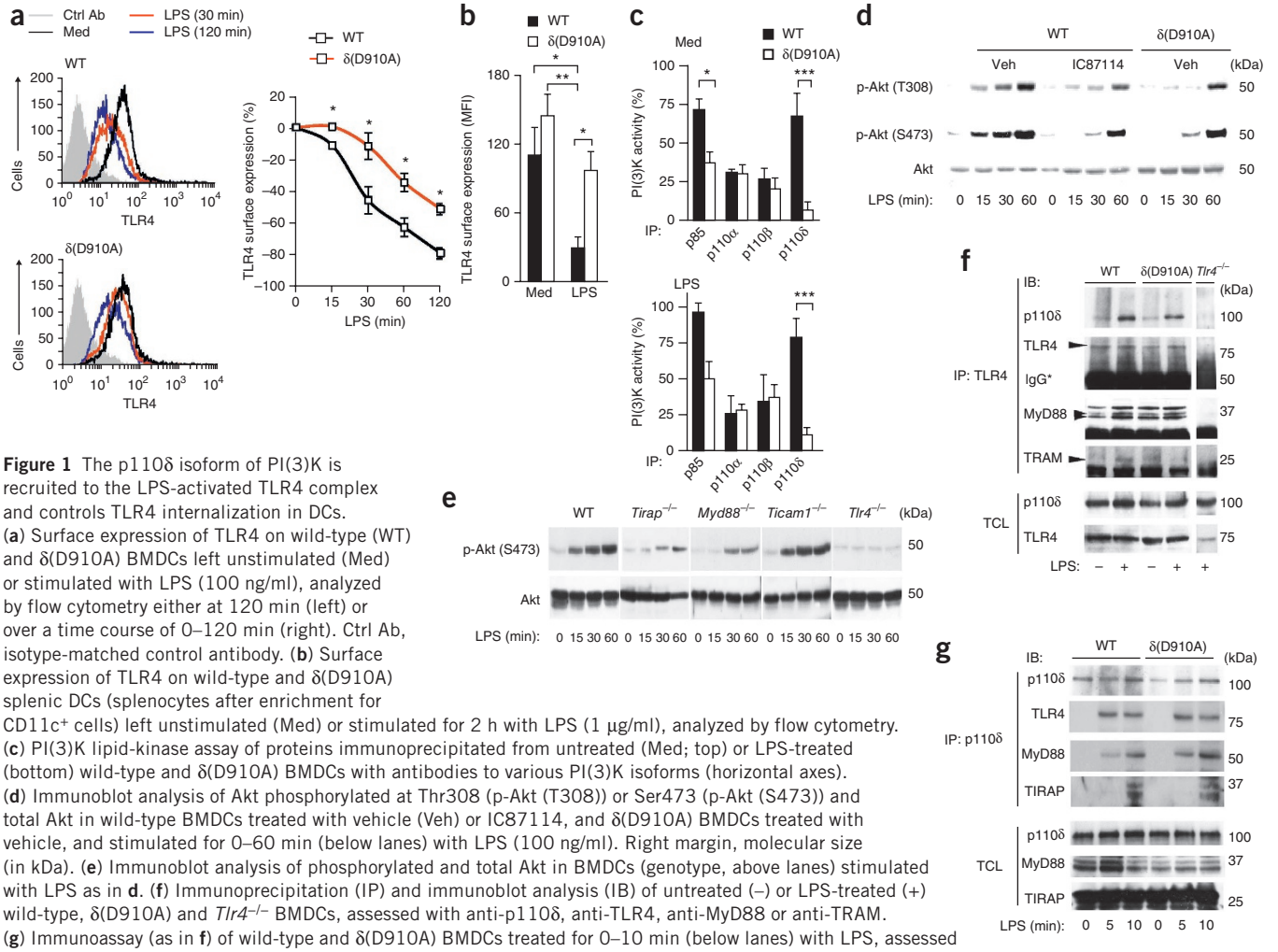

Figure 1 The p110δ isoform of PI(3)K is recruited to the LPS-activated TLR4 complex and controls TLR4 internalization in DCs. (**a**) Surface expression of TLR4 on wild-type (WT) and δ(D910A) BMDCs left unstimulated (Med) or stimulated with LPS (100 ng/ml), analyzed by flow cytometry either at 120 min (left) or over a time course of 0–120 min (right). Ctrl Ab, isotype-matched control antibody. (**b**) Surface expression of TLR4 on wild-type and δ(D910A) splenic DCs (splenocytes after enrichment for CD11c$^+$ cells) left unstimulated (Med) or stimulated for 2 h with LPS (1 μg/ml), analyzed by flow cytometry. (**c**) PI(3)K lipid-kinase assay of proteins immunoprecipitated from untreated (Med; top) or LPS-treated (bottom) wild-type and δ(D910A) BMDCs with antibodies to various PI(3)K isoforms (horizontal axes). (**d**) Immunoblot analysis of Akt phosphorylated at Thr308 (p-Akt (T308)) or Ser473 (p-Akt (S473)) and total Akt in wild-type BMDCs treated with vehicle (Veh) or IC87114, and δ(D910A) BMDCs treated with vehicle, and stimulated for 0–60 min (below lanes) with LPS (100 ng/ml). Right margin, molecular size (in kDa). (**e**) Immunoblot analysis of phosphorylated and total Akt in BMDCs (genotype, above lanes) stimulated with LPS as in **d**. (**f**) Immunoprecipitation (IP) and immunoblot analysis (IB) of untreated (–) or LPS-treated (+) wild-type, δ(D910A) and *Tlr4*$^{-/-}$ BMDCs, assessed with anti-p110δ, anti-TLR4, anti-MyD88 or anti-TRAM. (**g**) Immunoassay (as in **f**) of wild-type and δ(D910A) BMDCs treated for 0–10 min (below lanes) with LPS, assessed with anti-p110δ, anti-TLR4, anti-MyD88 or anti-TIRAP. $*P < 0.01$, $**P < 0.001$ and $***P < 0.0001$ (Student's *t*-test). Data represent one of three experiments (**a**; mean ± s.d. (right) of three to four mice per group), four experiments (**b**; mean and s.d. of three to four mice per group), three experiments (**c**; mean and s.d. of three mice per group), one of three experiments (**d**,**e**) or at least two experiments with two to three mice per group (**f**,**g**).

© 2012 Nature America, Inc. All rights reserved.

plasma membrane ruffles, which were enriched for PtdIns(4,5)P_2 (**Fig. 2a**), in line with published observations[3]. We also visualized a detectable fraction of TIRAP in intracellular locations that overlapped with the PtdIns(4,5)P_2 staining in cells from both genotypes (**Fig. 2a**). After 20 min of stimulation of wild-type BMDCs with LPS, a large proportion of TIRAP had dissociated from the plasma membrane ruffles, followed by an overall decrease in TIRAP staining within 1 h both at the plasma membrane and in cytosolic compartments (**Fig. 2a–c**). Under both basal and LPS-stimulated conditions at 10 min or 1 h, TIRAP did not localize together with the early endosomal antigen EEA1 (**Supplementary Fig. 3** and data not shown), which indicated that TIRAP was not internalized to early endosomes in either wild-type or δ(D910A) cells.

Unlike its positioning in wild-type cells, TIRAP in δ(D910A) BMDCs persisted at the plasma membrane for up to 20 min after LPS stimulation (**Fig. 2a**,**c**). We also observed similar retention of TIRAP at the plasma membrane in IC87114-treated wild-type cells and in δ(D910A) BMDCs stimulated with LPS, with some TIRAP still detectable at the plasma membrane as late as at 1 h after LPS stimulation (**Fig. 2b**,**c** and data not shown). These data showed that inactivation of p110δ delayed the LPS-induced dissociation of TIRAP from the plasma membrane.

Next we transiently transfected wild-type and δ(D910A) BMDCs to express green fluorescent protein (GFP)-tagged TIRAP and visualized these cells by confocal microscopy. These experiments confirmed the finding that LPS activation of wild-type cells resulted in time-dependent, rapid loss of GFP-TIRAP from the plasma membrane and also from the cytosol (**Fig. 2d**). In a similar setting in LPS-activated δ(D910A) cells, GFP-TIRAP persisted for up to 30 min with very little loss of TIRAP from the plasma membrane (**Fig. 2d**). Biochemical fractionation of membrane and cytosolic compartments provided further evidence that inhibition of p110δ prolonged the residence of TIRAP at the plasma membrane after activation by LPS. Under basal conditions, the membrane fraction showed enrichment for TIRAP, with some TIRAP redistributed to the cytosol 15 min after stimulation with LPS (**Fig. 2e**). However, in δ(D910A) cells, little or no TIRAP redistributed to the cytosol after stimulation with LPS (**Fig. 2e**).

Proteins with polybasic regions can bind PtdIns(4,5)P_2 in a concentration-dependent manner and act as PtdIns(4,5)P_2 sensors[24]. In a protein-lipid overlay assay, a control protein generated by the fusion of glutathione *S*-transferase (GST) and phospholipase C-δ–pleckstrin homology domain (PLC-δ-PH, which has a known 'preference' for PtdIns(4,5)P_2)[25] and recombinant GST-TIRAP interacted more effectively with PtdIns(4,5)P_2 than did GST–Akt-PH (used as

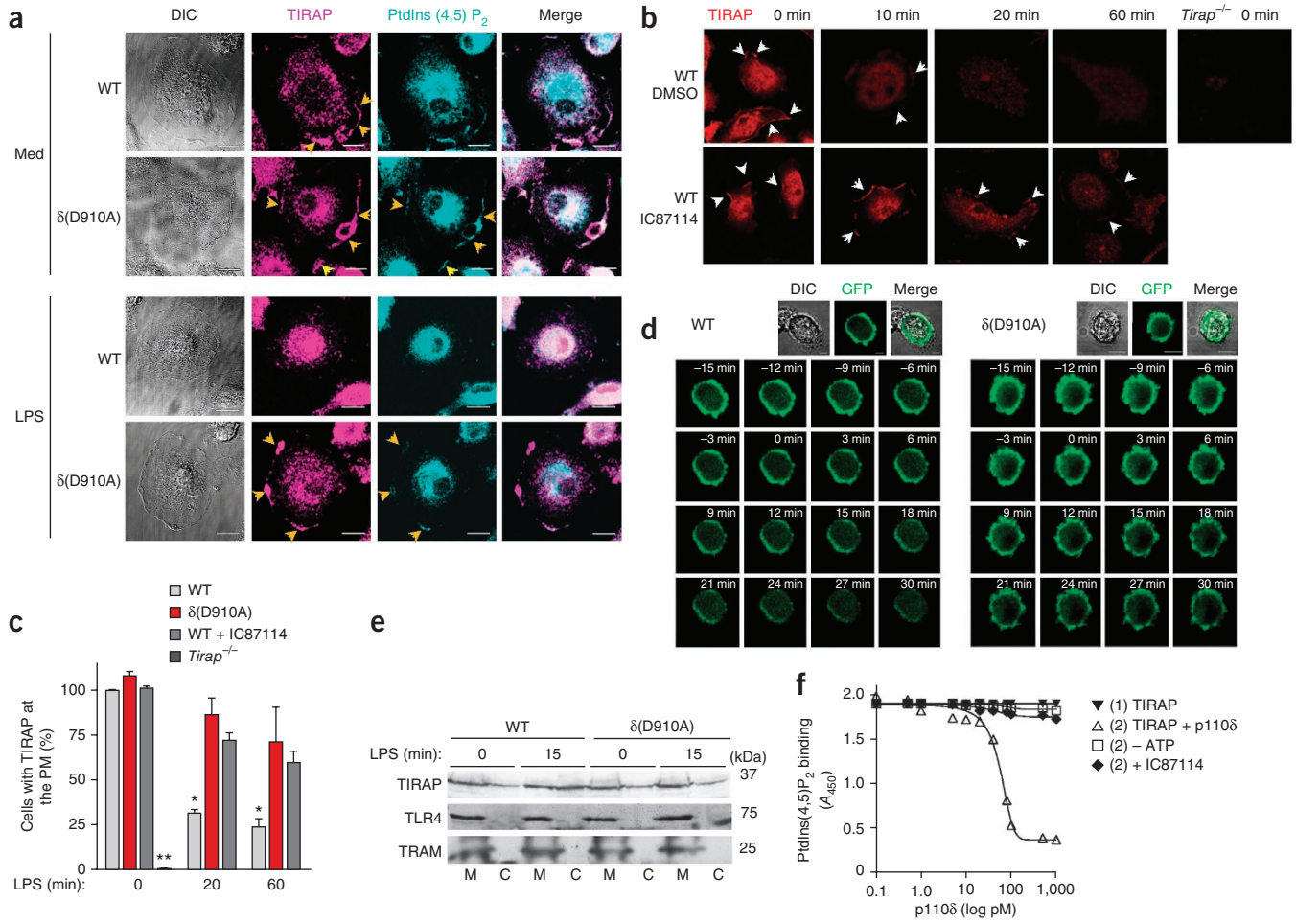

Figure 2 The activity of p110δ in BMDCs is involved in the dissociation of TIRAP from the plasma membrane after stimulation with LPS. (**a**) Confocal microscopy of wild-type and δ(D910A) BMDCs left untreated (Med) or activated for 20 min with LPS and then stained with anti-TIRAP or GST–PLC-δ-PH, followed by anti-GST (to probe for PtdIns(4,5)P_2); arrowheads indicate the localization of TIRAP with PtdIns(4,5)P_2 at the plasma membrane. DIC, differential interference contrast. Scale bars, 10 μm. (**b**) Confocal microscopy of wild-type BMDCs (left group) pretreated for 1 h with vehicle (DMSO) or IC87114 (1 μM) and then stimulated for 0–60 min (above images) with LPS (100 ng/ml), and of a *Tirap*$^{-/-}$ BMDC treated with vehicle and left unstimulated (far right). Arrowheads indicate localization of TIRAP at the cell periphery. Original magnification, ×63. (**c**) Frequency of BMDCs (n = 50–60, collected from ten fields) with TIRAP staining at the plasma membrane, assessed by differential interference contrast microscopy (treated, stained and analyzed as in **a**,**b**). *P < 0.01 and **P < 0.001 (Student's t-test). (**d**) Video microscopy of wild-type and δ(D910A) BMDCs transfected to express GFP-TIRAP and then imaged for 15 min in medium alone before stimulation with LPS (100 ng/ml), followed by imaging for 18 h (time, top right corners; '0 min' indicates 1 min after the addition of LPS). Original magnification, ×63. (**e**) Immunoblot analysis of lysates of wild-type and δ(D910A) BMDCs stimulated for 0 or 15 min with LPS (100 ng/ml), followed by subcellular fractionation of the membrane (M) and cytosol (C). (**f**) PI(3)K kinase assay of the binding of PtdIns(4,5)P_2 to TIRAP in plates coated with PtdIns(4,5)P_2 and preincubated with GST-TIRAP, followed by the addition of TIRAP alone ((1) TIRAP), TIRAP plus recombinant p110δ-p85 fusion protein ((2) TIRAP + p110δ), TIRAP plus p110δ-p85 without ATP ((2) – ATP) and TIRAP plus p110δ-p85 preincubated with IC87114 (1 μM) ((2) + IC87114)); results are presented as absorbance at 450 nm (A_{450}). Data are from one experiment with five mice per group (**a**; one image of at least ten per condition), one experiment representative of three (**b**,**e**,**f**; with triplicates in **f**) or three experiments with two to three mice per strain (**c**; mean and s.d.) or two mice per strain (**d**; one image of at least two to three per condition).

a probe for PtdIns(3,4,)P_2 and PtdIns(3,4,5)P_3) or GST–Hrs-FYVE (a fusion of GST and the FYVE zinc-finger domain derived from the endosome-associated protein Hrs, used as a probe for for PtdIns(3)P), as described before[26,27] (**Supplementary Fig. 4a**). Moreover, in an *in vitro* lipid-vesicle–association assay, TIRAP and PLC-δ-PH had a sigmoidal PtdIns(4,5)P_2 concentration–dependent binding pattern (**Supplementary Fig. 4b**), with TIRAP binding less effectively than PLC-δ-PH, in line with stronger affinity of the latter for PtdIns(4,5)P_2, even at low concentrations[25]. In protein-lipid overlay assays, TIRAP effectively bound to PtdIns(4,5)P_2, but TIRAP-4x, a mutant version of TIRAP lacking the four lysine residues in its polybasic domain[3], did not (**Supplementary Fig. 4c**). In a similar assay in the presence of ATP, recombinant p110δ diminished the binding of TIRAP to PtdIns(4,5)P_2 in a dose-dependent way, an effect that was blocked by IC87114 or removal of ATP from the reaction buffer (**Fig. 2f**); this indicated that p110δ diminished the binding of TIRAP to PtdIns(4,5)P_2 mainly through its lipid-kinase activity. These data indicated that p110δ was able to compete with and derease the binding of TIRAP to PtdIns(4,5)P_2 *in vitro*.

We obtained additional evidence that the kinase activity of p110δ can control the localization of TIRAP through the regulation of PtdIns(4,5)P_2-PtdIns(3,4,5)P_3 dynamics from a cell-based model with NIH3T3 mouse fibroblasts, which lack detectable endogenous p110δ expression[12] (**Supplementary Fig. 5a**). Stable expression in

© 2012 Nature America, Inc. All rights reserved.

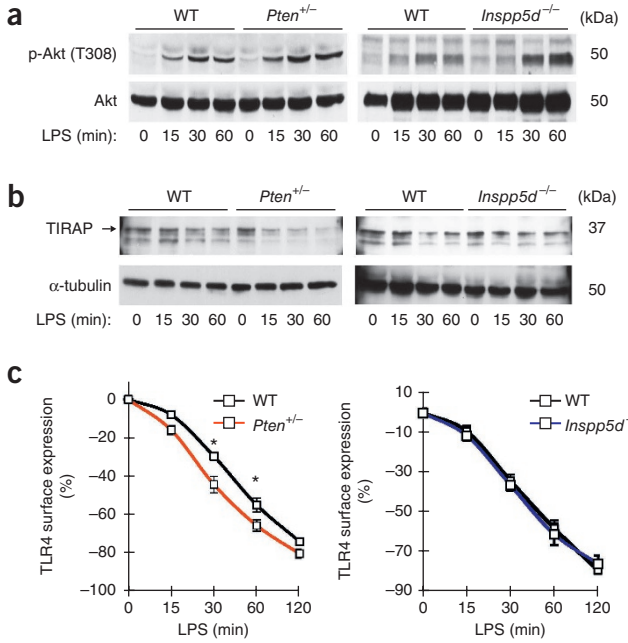

Figure 3 PTEN regulates LPS-induced TIRAP degradation and TLR4 internalization in BMDCs, but SHIP does not. (**a**) Immunoblot analysis of phosphorylated and total Akt in wild-type, *Pten*$^{+/-}$ and SHIP-1-deficient (*Inpp5d*$^{-/-}$) BMDCs treated for 0–60 min (below lanes) with LPS (100 ng/ml). (**b**) Immunoblot analysis of TIRAP and α-tubulin (loading control) in lysates of wild-type, *Pten*$^{+/-}$ and SHIP-1-deficient BMDCs treated for 0–60 min (below lanes) with LPS. (**c**) Surface expression of TLR4 on wild-type, *Pten*$^{+/-}$ and SHIP-1-deficient BMDCs stimulated for 0–120 min (horizontal axis) with LPS (100 ng/ml), analyzed by flow cytometry. $^{*}P < 0.01$ (Student's *t*-test). Data are from one experiment representative of three (**a**), one experiment representative of two with three to four mice per group (**b**) or three experiments (**c**; mean ± s.d. of three mice per group).

these cells of a membrane-targeted version of p110δ resulted in a greater abundance of PtdIns(3,4,5)P_3 (**Supplementary Fig. 5b**) and constitutive phosphorylation of Akt (**Supplementary Fig. 5a**). In line with the conversion of PtdIns(4,5)P_2 to PtdIns(3,4,5)P_3 by the membrane-targeted version of p110δ, there was depletion of TIRAP from the plasma membrane borders (**Supplementary Fig. 5b**,**c**) with notably less TIRAP protein expression overall (**Supplementary Fig. 5a**). The localization and abundance of TIRAP were not altered after expression of empty-control vector or wild-type p110δ (**Supplementary Fig. 5a**,**b** and data not shown). Together these data confirmed that the interaction of TIRAP with PtdIns(4,5)P_2 was abolished by the kinase activity of p110δ.

Activity of p110δ facilitates proteolysis of TIRAP by calpain

Degradation of TIRAP after stimulation of LPS is a fast way to terminate TIRAP-MyD88–dependent signaling[28]. The prolonged presence of TIRAP at the plasma membrane of δ(D910A) BMDCs and lower abundance of TIRAP protein in LPS-stimulated BMDCs and in NIH3T3 cells expressing constitutively active p110δ suggested that p110δ might affect LPS-induced degradation of TIRAP. In wild-type BMDCs, TIRAP was gradually processed and disappeared within 1 h after LPS stimulation (**Fig. 3a** and **Supplementary Fig. 6a**). In contrast, δ(D910A) BMDCs and IC87114-pretreated wild-type cells showed little or no degradation of TIRAP at 20 min after LPS stimulation, with some degradation observed 1 h after LPS stimulation (**Fig. 3a** and **Supplementary Fig. 6a**). We obtained similar results with IC87714-treated J774 mouse macrophages (**Supplementary Fig. 6a**,**b**). The PLC-γ inhibitor U73122 inhibited the LPS-induced degradation of TIRAP (**Supplementary Fig. 6a**), with the combination of IC87114 and U73112 resulting more TIRAP than noted after treatment with either inhibitor alone (**Supplementary Fig. 6a**). Notably, inhibition of endocytosis of TLR4 (with Dynasore[4], an inhibitor of the dynamin GTPase) did not prevent TIRAP degradation (**Supplementary Fig. 6a**). This suggested that depletion of PtdIns(4,5)P_2 at the plasma membrane and concomitant relocation of TIRAP to the cytosol were a precondition for the degradation of TIRAP.

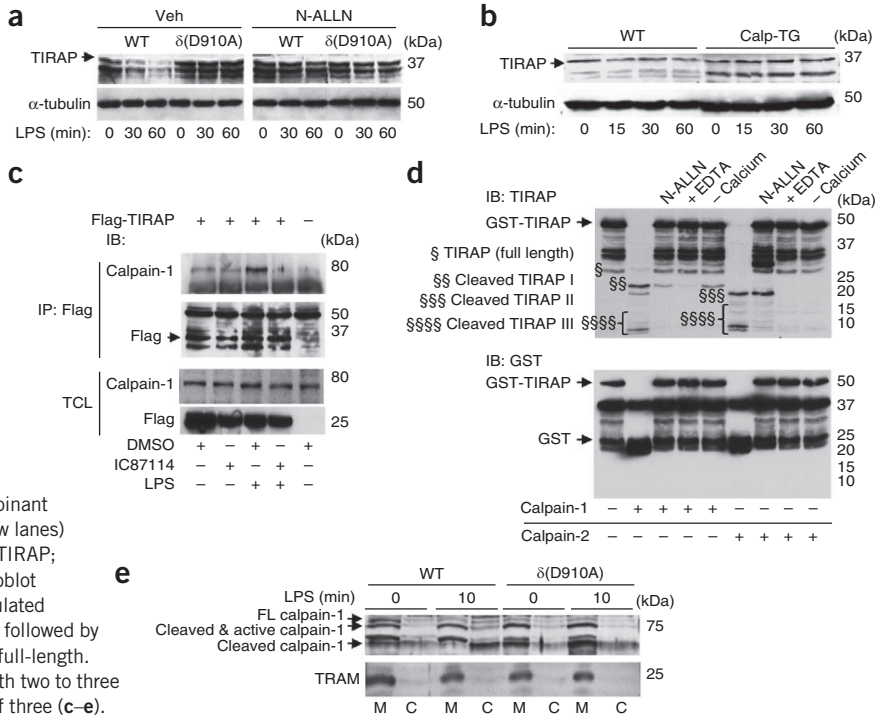

Figure 4 'Licensing' of calpain-induced TIRAP proteolysis by p110δ in BMDCs and J774 macrophages. (**a**) Immunoblot analysis of TIRAP and α-tubulin in lysates of wild-type and δ(D910A) BMDCs pretreated for 1 h with vehicle or N-ALLN (50 μM) and then activated for 0–60 min (below lanes) with LPS (100 ng/ml). (**b**) Immunoblot analysis of TIRAP and α-tubulin in lysates of wild-type BMDCs and BMDCs with transgenic expression of calpastatin (calp-TG), treated for 0–60 min (below lanes) with LPS. (**c**) Immunoprecipitation and immunoblot analysis of J774 macrophages left untransfected (–) or transfected for 36 h to express Flag-tagged TIRAP (+), then pretreated for 1 h with vehicle (DMSO) or IC87114 (1 μM) and then left unstimulated or stimulated for 10 min with LPS (1 μg/ml), assessed with anti-Flag or anti-calpain-1 (above), along with immunoblot analysis of total cell lysates (TCL; below). (**d**) Immunoblot analysis of recombinant GST-TIRAP incubated with calpain-1 or calpain-2 (below lanes) in various assay conditions (above lanes). §, full-length TIRAP; §§, §§§ and §§§§, TIRAP cleavage products. (**e**) Immunoblot analysis of wild-type and δ(D910A) BMDCs left unstimulated (0 min) or stimulated for 10 min with LPS (100 ng/ml), followed by subcellular fractionation of membrane and cytosol. FL, full-length. Data are from one experiment representative of three with two to three mice per group (**a**,**b**) or one experiment representative of three (**c**–**e**).

© 2012 Nature America, Inc. All rights reserved.

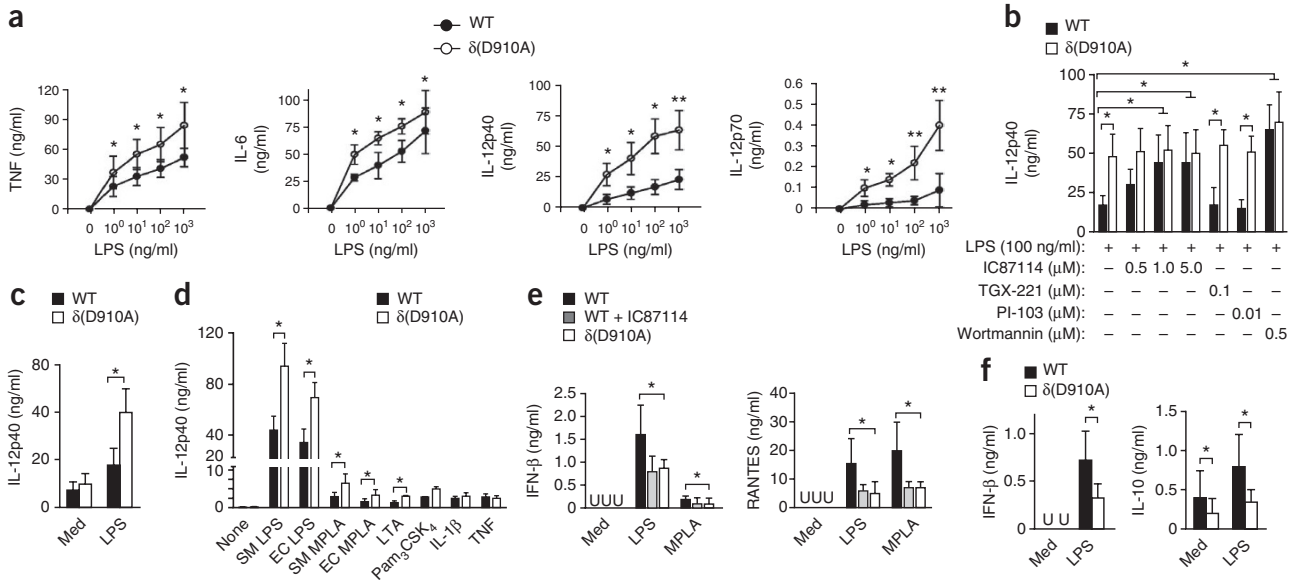

Figure 5 Inhibition of p110δ in BMDCs augments the production of proinflammatory cytokines while inhibiting IFN-β and the products of interferon-stimulated genes. (**a**) Cytokine concentrations in supernatants of wild-type and δ(D910A) BMDCs stimulated for 24 h with various concentrations of LPS (horizontal axes). $^*P < 0.05$ and $^{**}P < 0.005$ (Mann-Whitney *U*-test). (**b**) IL-12p40 concentrations in culture supernatant of wild-type and δ(D910A) BMDCs pretreated for 1 h with various PI(3)K inhibitors (below), followed by stimulation for 24 h with LPS (100 ng/ml). $^*P < 0.05$ (Mann-Whitney *U*-test). (**c**) IL-12p40 concentration in supernatants of wild-type and δ(D910A) splenocytes left unstimulated (Med) or stimulated with LPS (100 ng/ml). $^*P < 0.05$ (Mann-Whitney *U*-test). (**d**) IL-12p40 concentration in wild-type and δ(D910A) BMDCs left unstimulated (None) or stimulated with various TLR ligands (horizontal axis) or IL-1β (20 ng/ml) or TNF (20 ng/ml). SM, *S. minnesota*; EC, *E. coli*; MPLA, monophosphoryl lipid A; LTA, lipoteichoic acid. $^*P < 0.05$ (Mann-Whitney *U*-test). (**e**) Concentration of IFN-β and RANTES in supernatant of wild-type and δ(D910A) BMDCs, as well as wild-type BMDCs treated with IC87114 (0.5 μM; WT + IC87114), left unstimulated (Med) or stimulated with LPS or monophosphoryl lipid A. U, undetectable. $^*P < 0.05$ (analysis of variance). (**f**) Concentration of IFN-β and IL-10 in supernatants of wild-type and δ(D910A) splenocytes left unstimulated (Med) or stimulated with LPS (100 ng/ml). $^*P < 0.05$ (Mann-Whitney *U*-test). Data are representative of three experiments (**a**–**d**; mean ± s.d. of five mice per group in **a**; mean and s.d. of five to six mice per group in **b**; mean and s.d. in **c**; and mean and s.d. of five mice per group in **d**) or two experiments (**e**,**f**; mean and s.d. of five mice per group (**e**) or five to six mice per group (**f**)).

To further investigate the influence of acute changes in the ratio of PtdIns(4,5)P_2 to PtdIns(3,4,5)P_3 on LPS-induced TIRAP turnover and TLR4 internalization, we investigated LPS signaling in BMDCs with loss of function of the PtdIns(3,4,5)P_3 phosphatases PTEN or SHIP-1. The 3-phosphatase PTEN converts PtdIns(3,4,5)P_3 to PtdIns(4,5)P_2 and is reported to be a positive regulator of LPS-induced TLR4 signaling and secretion of proinflammatory cytokines through unknown mechanisms[29,30], whereas the 5-phosphatase SHIP-1 converts PtdIns(3,4,5)P_3 to PtdIns(3,4)P_2 (ref. 31) and negatively regulates the LPS-mediated production of proinflammatory mediators as well as of IFN-β[32,33]. There was more LPS-induced phosphorylation of Akt in BMDCs from either mutant mouse strain than in wild-type control cells, with baseline Akt phosphorylation being slightly greater in *Pten*$^{+/-}$ BMDCs but not in SHIP-1-deficient BMDCs (**Fig. 3a**). The kinetics of LPS-induced degradation of TIRAP were faster in *Pten*$^{+/-}$ BMDCs than in wild-type control cells, with no substantial difference between SHIP-1-deficient and wild-type cells (**Fig. 3b**). The surface expression of TLR4 was similar in BMDCs from both strains, with faster LPS-induced internalization of TLR4 in *Pten*$^{+/-}$ BMDCs than in wild-type cells but similar kinetics of TLR4 internalization in SHIP-1-deficient cells and their wild-type counterparts (**Fig. 3c**). Overall, these data supported the idea that PtdIns(4,5)P_2–PtdIns(3,4,5)P_3 dynamics, rather than a greater abundance of PtdIns(3,4,5)P_3 itself, controlled both TLR4 internalization and the degradation kinetics of TIRAP.

TIRAP degradation involves the ubiquitin-proteasome pathway[28]. In line with that, the proteasome inhibitor MG-132 abolished the degradation of TIRAP after LPS stimulation in BMDCs and in J774 macrophages (**Supplementary Fig. 6a**,**b**). As cytosolic TIRAP may also be susceptible to the action of calpain, a ubiquitously expressed nonlysosomal cysteine protease[34], we assessed the calpain inhibitor N-ALLN and found that it abolished LPS-induced degradation of TIRAP in wild-type and δ(D910A) BMDCs and in J774 cells (**Fig. 4a** and **Supplementary Fig. 6a**,**b**). LPS-induced degradation of TIRAP was also inhibited in BMDCs derived from mice with transgenic overexpression of calpastatin, the endogenous inhibitor of calpain-1 and calpain-2 (ref. 35; **Fig. 4b**). We transfected J774 cells to express Flag-tagged TIRAP and found that it immunoprecipitated together with calpain-1 under both basal and LPS-activated conditions, and that treatment with IC87114 resulting in less interaction (**Fig. 4c**). We confirmed those results by finding that recombinant GST-TIRAP was efficiently cleaved and processed *in vitro* by purified calpain-1 and calpain-2 in a calcium-dependent and N-ALLN-sensitive manner (**Fig. 4d**). Calpain-1 activity is regulated by autoprocessing of the large 80-kilodalton (kDa) subunit into a cleaved and active form 78–76 kDa in size, which is then detached from the plasma membrane to the cytosolic compartment[34]. Cell-fractionation assays of BMDCs showed that the membrane fraction contained most of the full-length calpain-1 (80 kDa), which, after 10 min of stimulation with LPS, was cleaved into a 78- to 76-kDa fragment and then translocated to the cytosolic fraction (**Fig. 4e**). In δ(D910A) BMDCs, the translocation to the cytosol and cleavage of calpain-1 was considerably inhibited (**Fig. 4e**). Together these data indicated that the sequential action of calpain proteases and proteasome in the cytosol most probably led to the proteolysis of TIRAP and that p110δ activity also controlled the localization of calpain-1 to the cytosol after activation by LPS.

© 2012 Nature America, Inc. All rights reserved.

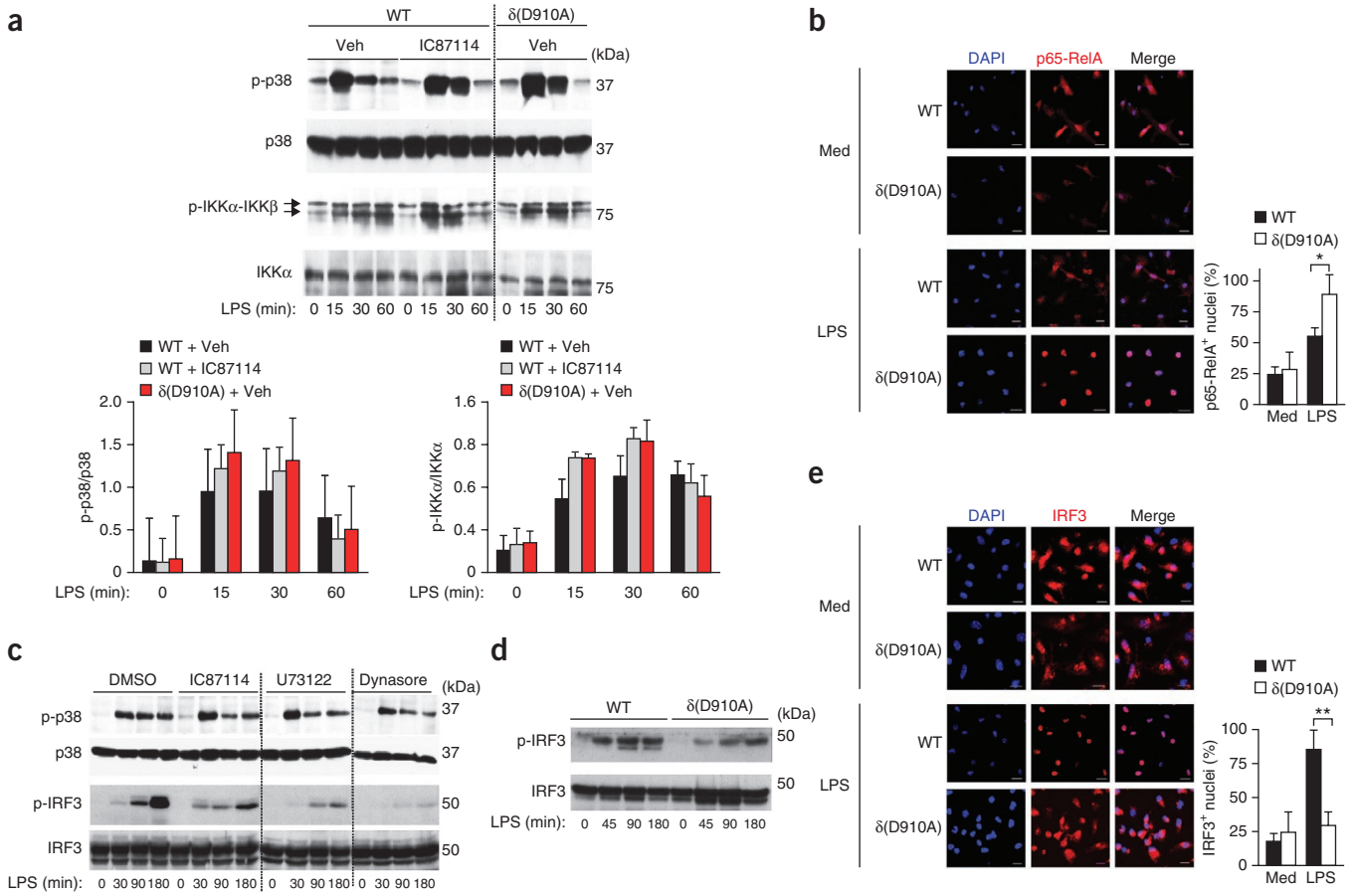

Figure 6 The kinase activity of p110δ in BMDCs is required for optimal IFN-β production through IRF3 and late activation of NF-κB and p38. (**a**) Immunoblot analysis (top) of phosphorylated and total p38 and IKKα-IKKβ in extracts of wild-type BMDCs treated with vehicle (Veh) or IC87114, and δ(D910A) BMDCs treated with vehicle, stimulated for 0–60 min (below lanes) with LPS (100 ng/ml); below, ratio of phosphorylated protein to total protein. Vertical dotted line (top) indicates cropped lanes compiled from immunoblots of lysates analyzed simultaneously under the same conditions. (**b**) Confocal microscopy (left) of wild-type and δ(D910A) BMDCs left unstimulated or stimulated for 45 min with LPS (100 ng/ml), stained with the DNA-intercalating dye DAPI (staining nuclei) and for NF-κB p65 (p65-RelA); and frequency of BMDCs with only p65$^+$ nuclei ($n = 50$ cells for each of three mice per group; right). Scale bars (left), 10 μm. $^*P < 0.01$ (Student's *t*-test). (**c**) Immunoblot analysis of phosphorylated and total p38 and IRF3 in wild-type BMDCs treated with vehicle (DMSO), IC87114, U73221 or Dynasore, then stimulated for 0–180 min with LPS (10 ng/ml). Vertical dotted lines, as in **a**. (**d**) Immunoblot analysis of phosphorylated and total IRF3 in wild-type and δ(D910A) BMDCs stimulated for 0–180 min with LPS (10 ng/ml). (**e**) Confocal microscopy (left) of IRF3 and DAPI staining in BMDCs as in **b**; and frequency of BMDCs with only IRF3$^+$ nuclei ($n = 50$ cells for each of three mice per group; right). Scale bars, 10 μm. $^{**}P < 0.01$ by Student's *t*-test (right). Data are from one representative of three experiments with three to four mice (**a**, top) or two to three experiments with two to three mice (**c**,**d**) or are representative of one experiment (**a**, bottom; mean and s.e.m. of three mice per group) or three experiments (**b**,**e**; mean and s.d.).

© 2012 Nature America, Inc. All rights reserved.

npg

PI(3)K p110δ regulates TLR4 signaling pathways differently

PI(3)K is reported to be a negative regulator of LPS-mediated production of proinflammatory cytokines in DCs, based on studies of p85-deficient BMDCs[16]. However, the roles of the catalytic isoforms of class I PI(3)Ks in TLR4 signaling have remained enigmatic. After stimulation with LPS, but not under basal conditions, the production of tumor-necrosis factor (TNF), IL-6, IL-12p40 and IL-12p70 was significantly greater in δ(D910A) BMDCs than in wild-type cells (**Fig. 5a**), an effect we did not observe after genetic inactivation of p110α or p110β (**Supplementary Fig. 7a,b**). We noted a similar enhancement after pretreatment of LPS-stimulated wild-type BMDCs with IC87114 or pan-PI(3)K inhibitors (wortmannin or LY294002) but not after pretreatment with inhibitors with selectivity for p110α (PI-103), p110β (TGX-221) or p110γ (AS604850) (**Fig. 5b** and data not shown). Notably, IC87114 did not further enhance cytokine expression in LPS-activated δ(D910A) cells (**Fig. 5b**). Likewise, we observed amplified production of inflammatory cytokines in δ(D910A) splenocytes relative to their production in wild-type control cells (**Fig. 5c**). Inhibition of p110δ activity also amplified inflammatory responses induced by other TLR ligands that signal through TIRAP, as shown by the enhanced IL-12p40 production after inhibition of p110δ in BMDCs stimulated with the TLR4 ligand monophosphoryl lipid A (from *E. coli* or purified *Salmonella minnesota* R595) or by TLR2-specific ligands such as lipoteichoic acid and the tripalmitoylated lipopeptide PAM_3SCK_4 (**Fig. 5d**). Signaling through the receptors for IL-1 or TNF, which do not use TIRAP, was not affected by inactivation of p110δ (**Fig. 5d**).

Endosomal TRAM-TRIF signaling activates IRF3 that gives rise to IFN-β and the downstream products of interferon-stimulated genes, including RANTES and IL-10 (refs. 36–38). In line with less internalization of TLR4, genetic or pharmacological inactivation of p110δ (but not of p110α or p110β) resulted in less production of IFN-β in LPS-stimulated BMDCs (**Fig. 5e** and data not shown). Less IFN-β and IL-10 was produced by LPS-activated δ(D910A) splenic DCs than

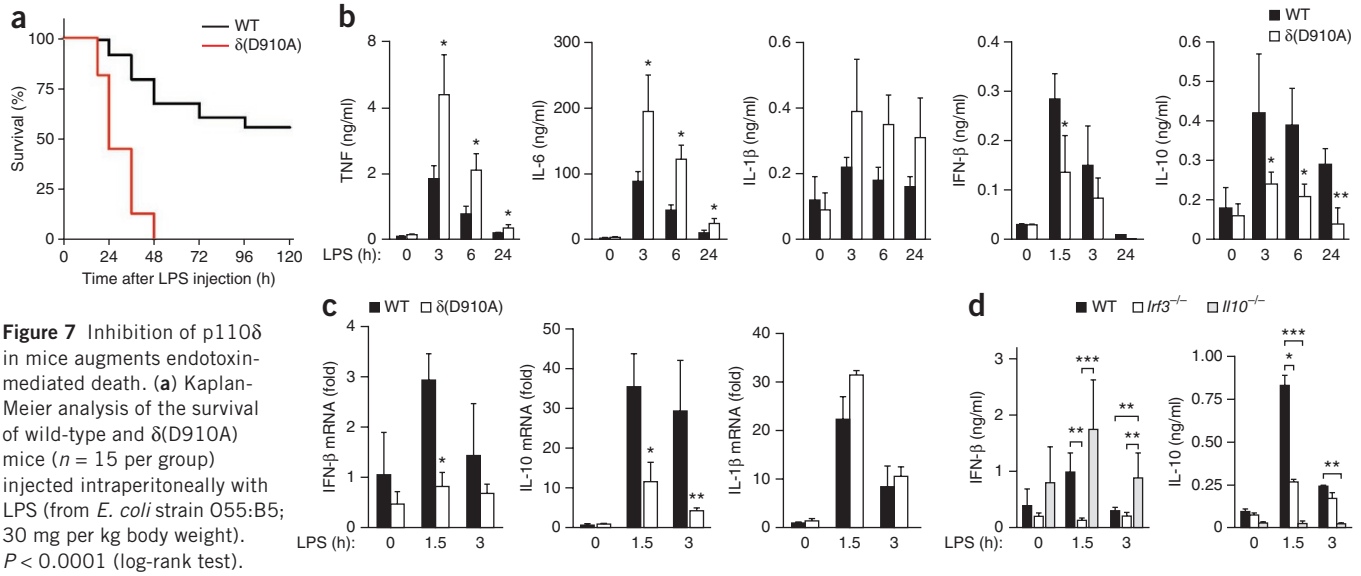

Figure 7 Inhibition of p110δ in mice augments endotoxin-mediated death. (**a**) Kaplan-Meier analysis of the survival of wild-type and δ(D910A) mice ($n = 15$ per group) injected intraperitoneally with LPS (from *E. coli* strain 055:B5; 30 mg per kg body weight). $P < 0.0001$ (log-rank test). (**b**) Cytokine concentrations in serum from mice treated as in **a**. $^{*}P < 0.05$ and $^{**}P < 0.005$ (Mann-Whitney *U*-test). (**c**) Cytokine mRNA in spleens of mice treated as in **a**, presented relative to the abundance of HPRT mRNA (encoding hypoxanthine guanine phosphoribosyl transferase). $^{*}P < 0.05$ and $^{**}P < 0.005$ (Mann-Whitney *U*-test). (**d**) Plasma concentration of IFN-β and IL-10 in serum from wild-type, IRF3- and IL-10-deficient mice injected intraperitoneally with LPS (from *E. coli* strain 0111:B4; 10 mg per kg body weight). $^{*}P < 0.05$, $^{**}P < 0.005$ and $^{***}P < 0.005$ (Mann-Whitney *U*-test). Data are representative of two experiments (mean and s.d. of three to five mice per group in **b**–**d**).

by their LPS-activated wild-type counterparts (**Fig. 5f**). In a similar setting, *Pten*$^{+/-}$ BMDCs had less LPS-induced production of TNF but unaffected production of IFN-β or slightly more production of IFN-β only at highest doses of LPS (**Supplementary Fig. 8a**,**b**). These results suggested that activation of p110δ induced IFN-β and anti-inflammatory IL-10 after internalization of TLR4 while dampening TIRAP-MyD88–mediated proinflammatory signaling.

The recognition of LPS by TLR4 induces biphasic activation of NF-κB and p38, with the initial signal originating at the plasma membrane via TIRAP-MyD88, followed by TRAM-TRIF later in the endosomes. LPS-stimulated phosphorylation of the kinases IKKα, IKKβ and p38 tended to be greater at early time points (15–30 min) in δ(D910A) BMDCs than in wild-type cells (**Fig. 6a**). Translocation of the NF-κB family member RelA (p65) was also greater at 45 min in LPS-stimulated δ(D910A) BMDCs than in wild-type cells, with no notable differences in unstimulated cells from either genotype (**Fig. 6b**).

We therefore predicted that interfering with the localization and/or stability of TIRAP would also affect the late phases of TLR4 signaling. Indeed, in a longer kinetic study, IC87114 and U73221 each enhanced the LPS-stimulated phosphorylation of p38 at 30 min but diminished its late-phase phosphorylation at 90 min (**Fig. 6c**), which indicated that inactivation of p110δ delayed endosomal signaling by TLR4. The dynamin GTPase inhibitor Dynasore inhibited LPS-stimulated phosphorylation of p38 in the late phase but had minimal effect on the early phase of signaling (**Fig. 6c**), indicative of a block only in the intracellular TLR4 signaling, similar to that observed in TRIF- or TRAM-deficient cells[2]. Phosphorylation of IRF3 at Ser396, which is required for its translocation to the nucleus, was much lower in cells treated with IC87114 or U73221 than in untreated cells (**Fig. 6c**), which indicated that p110δ and PLC-γ controlled the internalization of TLR4 and its endosomal signaling to IRF3. Dynasore also blocked LPS-induced phosphorylation of IRF3, reported before to inhibit RANTES production[4] (**Fig. 6c**). Furthermore, δ(D910A) BMDCs had much less LPS-induced phosphorylation of IRF3 at Ser396 (**Fig. 6d**) and its localization to the nucleus (**Fig. 6e**) than did wild-type cells. Together these data demonstrated that inactivation of p110δ amplified TIRAP-MyD88–dependent TLR4 signaling while dampening the MyD88-independent IRF3 pathway in endosomes.

PI(3)K p110δ confers protection from endotoxin shock *in vivo*

To evaluate the *in vivo* pathobiological relevance of the inactivation of p110δ in LPS signaling, we assessed systemic inflammation induced by a lethal dose of LPS in wild-type and δ(D910A) mice. After LPS challenge, 50% of the δ(D910A) mice died within 48 h, whereas half of the wild-type mice survived for up to 120 h (**Fig. 7a**). That lower resistance of δ(D910A) mice to endotoxin correlated with higher LPS-induced serum concentrations of the proinflammatory cytokines TNF, IL-6 and IL-1β (**Fig. 7b**), which are known to contribute to the lethal pathology at the early stages of endotoxin shock[39]. In contrast, δ(D910A) mice had lower expression of IFN-β and IL-10, a well-established downstream target of the IRF3–IFN-β axis[38,40] (**Fig. 7b**,**c**).

Our data indicated that p110δ activity restrained LPS-mediated systemic inflammation. We therefore explored whether the lower production of IFN-β and IL-10 observed in δ(D910A) mice originated from impaired activation of IRF3. After challenge with LPS, IRF3-deficient mice had much less synthesis of IFN-β and IL-10 mRNA and expression of IFN-β and IL-10 protein without a substantial effect on the transcription of *Tnf* or *Il1b* (**Fig. 7d** and data not shown). These data indicated that p110δ positively regulated the IRF3–IFN-β–IL-10 axis and its anti-inflammatory action during endotoxemia. Together these data indicated that the kinase activity of p110δ protected mice from endotoxin-induced death by preventing uncontrolled systemic inflammation.

DISCUSSION

Compartmentalization of TLR signaling is critical for the quantitative and qualitative outcome of the immune response after pathogen recognition[7]. In this study, we identified the p110δ isoform of PI(3)K

© 2012 Nature America, Inc. All rights reserved.

as a key intermediary molecule that facilitated the transition from a TIRAP-MyD88–dependent proinflammatory phase to a TRAM-TRIF–dependent anti-inflammatory phase of TLR4 signaling. A role for PI(3)K in negatively regulating TLR-mediated inflammatory signaling has been documented and was considered to be mediated in part through the Akt-mTOR-Foxo1 signaling axis[18,41,42]. In this study, we identified the following additional mechanism of PI(3)K action: modulation of the 'topology' of TLR4 signaling by depletion of local PtdIns(4,5)P_2. This adds another layer to PI(3)K signaling in addition to the classic PtdIns(3,4,5)P_3-dependent activation of Akt and mTOR. The serine-threonine kinase mTOR is indeed important in both innate and adaptive immunity, and mTOR activity inhibits IL-12 production, whereas blocking mTOR enhances LPS-induced IL-12 production[43]. In both human and mouse plasmacytoid DCs, p110δ-mTOR signaling is required for type I IFN-α induced by TLR9 and TLR7 (refs. 44,45). Given that the kinetics of LPS-induced phosphorylation of the mTOR downstream targets p70-S6 kinase and S6 were similar in p110δ-null and wild-type BMDCs (data not shown), it is unlikely that the p110δ functions we documented here were mediated through mTOR.

Our study has established a link between PI(3)K signaling and surveillance for early endotoxic shock. We found that the internalization of LPS through TLR4 and the degradation of TIRAP coordinated by p110δ were key steps in dampening TIRAP-MyD88–dependent proinflammatory signaling to prevent fatal damage to the host. Although p110δ-null mice and TRAM- or TRIF-deficient mice were defective in generating type I IFN-β, only TRAM- or TRIF-deficient mice were also unable to generate proinflammatory cytokines. Therefore, inactivation of p110δ diminished but did not abrogate the interaction of activated TLR4 with TRAM. Similarly, inhibiting the Syk–PLC-γ2 signaling axis in BMDCs and macrophages results in less internalization of TLR4, which leads to inhibition of IFN-β production without affecting the abundance of proinflammatory cytokines[46], a phenotype reminiscent of that of p110δ-null mice. Thus, the kinase action of p110δ probably liberates TLR4 molecules to transit to the early endosomes, where they interact with TRAM, which leads to the induction of type I IFN-β. In this context, marshalling of the IFN-β–type I interferon receptor axis by p110δ via IL-10, after cessation of TIRAP-MyD88 signaling, is the second key step that 'revs up' a timely and effective anti-inflammatory arm of TLR4-mediated immune responses. Our study has identified p110δ in myeloid cells as a true homeostatic regulator of inflammation in endotoxic shock, which reinforces the proposal of an anti-inflammatory role for IFN-β[47–49]. Although the possibility of the involvement of DCs in the greater endotoxin-induced death δ(D910A) mice could be formally addressed by adoptive transfer *in vivo* of wild-type DCs or DC-specific inactivation of p110δ, it is unlikely that the DC phenotype is the sole cause of the observed phenotype. The p110δ isoform has high expression in all leukocytes, including macrophages[10], which also show enhanced LPS-induced responses[50], and these cells may therefore also be involved in the phenotype we have reported here for δ(D910A) mice. It is also possible that class I PI(3)K isoforms other than p110δ might control TLR4 signaling in other cell types in which p110δ concentrations are very low or it is absent[11].

To our knowledge, this is the first demonstration that changes in electrostatic interactions between PtdIns(4,5)P_2 and TLR adapters control the 'topology' of TLR4 signaling and influence the net outcome of systemic inflammation *in vivo*. Our data are in agreement with the 'electrostatic switch' model[6], as the net electrostatic force between membrane phospholipids and polybasic proteins can be diminished by signaling events (for example, by changes in membrane phospholipid composition or in the net charge of polybasic proteins (for example, by phosphorylation)). The resultant loss of attractive forces dissociates such proteins from membranes and is a way to rapidly compartmentalize signaling[23]. The localization of the polybasic molecules is influenced mainly by the concentration of the PtdIns(4,5)P_2 lipid, which is regulated dynamically in cells through synthesis, enzymatic conversion (through PLC-γ or PI(3)K) or clustering into spatial domains after occupancy by PtdIns(4,5)P_2-binding proteins. PtdIns(4,5)P_2 and PtdIns(3,4,5)P_3 lipids are important for vesicle uptake and transit, particularly during phagocytosis, in which both the PI(3)K product PtdIns(3,4,5)P_3 and PtdIns(3,4,5)P_3-mediated recruitment of PLC-γ have prominent roles[21]. The importance of PtdIns(4,5)P_2 binding for TIRAP function in immunity is substantiated by the observation that zebrafish, in which TIRAP lacks the PtdIns(4,5)P_2-binding polybasic motif, are insensitive to endotoxin[51]. Manipulation of the availability of PtdIns(4,5)P_2 is also a well-documented evolutionary strategy used by microorganisms such as *Salmonella typhimurium*, which have the phosphatidylinositol phosphatase SopB that dephosphorylates 4′- and 5′-phosphatidylinositols *in vivo* and allows depletion of cellular PtdIns(4,5)P_2 and disruption of the localization of TIRAP to the plasma membrane[52].

The PI(3)K-mediated control of the ratio of PtdIns(4,5)P_2 to PtdIns(3,4,5)P_3 and the calpain-ubiquitin-proteasome pathway may together represent a common regulatory mechanism that rapidly turns over proteins involved in spatiotemporal cell signaling. Calpain and the proteasome may act sequentially, similar to other calpain-regulated systems, partly by recognition of the Pro-Glu-Ser-Thr sequence on proteins[53,54], as overexpression of calpastatin in cells limits TIRAP degradation. Partial cleavage of TIRAP by calpain might therefore be the first processing step that earmarks TIRAP for subsequent full degradation by the ubiquitin-proteasome pathway[28].

Overall, our work has demonstrated the importance of correct compartmentalization of TLR signaling as a principle factor that defines the qualitative and quantitative output of innate immune responses that affect the fitness of the host to survive infection. In this context, the newly indentified link between PI(3)K activity and the IRF3–IFN-β–IL-10 pathway opens additional avenues to be exploited in the field of TLR biology, vaccine development and adjuvant-based immunotherapy to boost T helper type 1 immunity for the treatment of cancer and immunodeficiency generated by chronic viral infections.

METHODS

Methods and any associated references are available in the online version of the paper.

Note: Supplementary information is available in the online version of the paper.

ACKNOWLEDGMENTS

We thank R. Medzhitov (Yale University) for expression vectors encoding GST-TIRAP, GFP-TIRAP and GST–TIRAP-4x ; S. Akira (Osaka University) and L. O'Neill (Trinity College, Dublin) for TLR4-, MyD88-, TRIF- or TIRAP-deficient mice; L. Stephens (Babraham Institute) for SHIP-1-deficient mice; L. Baud (Hôpital Tenon) for mice with transgenic expression of calpastatin; G. Schiavo (London Cancer Research Institute) for the 2C11 mouse monoclonal antibody to PtdIns(4,5)P_2; T. Kinashi (Kyoto University) for the 5′ Myc membrane-targeted version of p110δ in the pMX-neo vector; T. Maffucci (Queen Mary, University of London) for GST–PLC-δ-PH and GST–Akt-PH; H. Stenmark (Oslo University Hospital) for GST–Hrs-FYVE; D. Gray (University of Edinburgh) for the XL-60 cell line; and B. Manoury, N. Leslie and members of the Centre for Cell Signalling for comments. Supported by the European Union Marie Curie (IEF-041713 to E.A. and IEF-274749 to S.T.); the European Molecular Biology Organization (ALTF 1083-2007 to E.A.); the Fondation ARC pour la Recherche sur la Cancer

© 2012 Nature America, Inc. All rights reserved.

(SAE P2009); the Fund for Scientific Research Flanders; the Hercules Foundation and University of Ghent Multidisciplinary Research Partnership (for work in the laboratory of R.B.); the European Union Marie Curie International Graduate Program in Molecular Medicine (M.A.W.); and Cancer Research UK (C23338/A10200), the Ludwig Institute for Cancer Research and Queen Mary University of London (for work in the laboratory of B.V.).

AUTHOR CONTRIBUTIONS

E.A. and B.V. developed the main hypothesis; E.A., S.T., D.T., S.D., A.H., W.P.P., I.M.B., G.N. and V.F. planned studies, did experiments and/or analyzed data; M.A.W., A.F. and R.B. contributed reagents, intellectual input and editorial assistance; E.A. and B.V. wrote the paper; B.V. supervised the project; and E.A. and B.V. obtained funding.

COMPETING FINANCIAL INTERESTS

The authors declare competing financial interests: details are available in the online version of the paper.

Published online at http://www.nature.com/doifinder/10.1038/ni.2426.
Reprints and permissions information is available online at http://www.nature.com/reprints/index.html.

© 2012 Nature America, Inc. All rights reserved.

1. Janeway, C.A. Jr. & Medzhitov, R. Innate immune recognition. *Annu. Rev. Immunol.* **20**, 197–216 (2002).
2. Akira, S. & Takeda, K. Toll-like receptor signalling. *Nat. Rev. Immunol.* **4**, 499–511 (2004).
3. Kagan, J.C. & Medzhitov, R. Phosphoinositide-mediated adaptor recruitment controls Toll-like receptor signaling. *Cell* **125**, 943–955 (2006).
4. Kagan, J.C. *et al.* TRAM couples endocytosis of Toll-like receptor 4 to the induction of interferon-beta. *Nat. Immunol.* **9**, 361–368 (2008).
5. Di Paolo, G. & De Camilli, P. Phosphoinositides in cell regulation and membrane dynamics. *Nature* **443**, 651–657 (2006).
6. McLaughlin, S., Wang, J., Gambhir, A. & Murray, D. PIP_2 and proteins: interactions, organization, and information flow. *Annu. Rev. Biophys. Biomol. Struct.* **31**, 151–175 (2002).
7. Barton, G.M. & Kagan, J.C. A cell biological view of Toll-like receptor function: regulation through compartmentalization. *Nat. Rev. Immunol.* **9**, 535–542 (2009).
8. Heo, W.D. *et al.* PI(3,4,5)P3 and PI(4,5)P2 lipids target proteins with polybasic clusters to the plasma membrane. *Science* **314**, 1458–1461 (2006).
9. Cantley, L.C. The phosphoinositide 3-kinase pathway. *Science* **296**, 1655–1657 (2002).
10. Vanhaesebroeck, B., Guillermet-Guibert, J., Graupera, M. & Bilanges, B. The emerging mechanisms of isoform-specific PI3K signalling. *Nat. Rev. Mol. Cell Biol.* **11**, 329–341 (2010).
11. Graupera, M. *et al.* Angiogenesis selectively requires the p110α isoform of PI3K to control endothelial cell migration. *Nature* **453**, 662–666 (2008).
12. Guillermet-Guibert, J. *et al.* The p110β isoform of phosphoinositide 3-kinase signals downstream of G protein-coupled receptors and is functionally redundant with p110γ. *Proc. Natl. Acad. Sci. USA* **105**, 8292–8297 (2008).
13. Hirsch, E. *et al.* Central role for G protein-coupled phosphoinositide 3-kinase γ in inflammation. *Science* **287**, 1049–1053 (2000).
14. Okkenhaug, K. *et al.* Impaired B and T cell antigen receptor signaling in p110δ PI 3-kinase mutant mice. *Science* **297**, 1031–1034 (2002).
15. Koyasu, S. The role of PI3K in immune cells. *Nat. Immunol.* **4**, 313–319 (2003).
16. Fukao, T. *et al.* PI3K-mediated negative feedback regulation of IL-12 production in DCs. *Nat. Immunol.* **3**, 875–881 (2002).
17. Guha, M. & Mackman, N. The phosphatidylinositol 3-kinase-Akt pathway limits lipopolysaccharide activation of signaling pathways and expression of inflammatory mediators in human monocytic cells. *J. Biol. Chem.* **277**, 32124–32132 (2002).
18. Brown, J., Wang, H., Suttles, J., Graves, D.T. & Martin, M. Mammalian target of rapamycin complex 2 (mTORC2) negatively regulates Toll-like receptor 4-mediated inflammatory response via FoxO1. *J. Biol. Chem.* **286**, 44295–44305 (2011).
19. Low, P.C. *et al.* Phosphoinositide 3-kinase δ regulates membrane fission of Golgi carriers for selective cytokine secretion. *J. Cell Biol.* **190**, 1053–1065 (2010).
20. Stephens, L., Ellson, C. & Hawkins, P. Roles of PI3Ks in leukocyte chemotaxis and phagocytosis. *Curr. Opin. Cell Biol.* **14**, 203–213 (2002).
21. Botelho, R.J. *et al.* Localized biphasic changes in phosphatidylinositol-4,5-bisphosphate at sites of phagocytosis. *J. Cell Biol.* **151**, 1353–1368 (2000).
22. Stauffer, T.P., Ahn, S. & Meyer, T. Receptor-induced transient reduction in plasma membrane PtdIns(4,5)P2 concentration monitored in living cells. *Curr. Biol.* **8**, 343–346 (1998).
23. Grinstein, S. Imaging signal transduction during phagocytosis: phospholipids, surface charge, and electrostatic interactions. *Am. J. Physiol. Cell Physiol.* **299**, C876–C881 (2010).
24. Papayannopoulos, V. *et al.* A polybasic motif allows N-WASP to act as a sensor of PIP_2 density. *Mol. Cell* **17**, 181–191 (2005).
25. Lemmon, M.A., Ferguson, K.M., O'Brien, R., Sigler, P.B. & Schlessinger, J. Specific and high-affinity binding of inositol phosphates to an isolated pleckstrin homology domain. *Proc. Natl. Acad. Sci. USA* **92**, 10472–10476 (1995).
26. Gray, A., Van Der Kaay, J. & Downes, C.P. The pleckstrin homology domains of protein kinase B and GRP1 (general receptor for phosphoinositides-1) are sensitive and selective probes for the cellular detection of phosphatidylinositol 3,4-bisphosphate and/or phosphatidylinositol 3,4,5-trisphosphate in vivo. *Biochem. J.* **344**, 929–936 (1999).
27. Gillooly, D.J. *et al.* Localization of phosphatidylinositol 3-phosphate in yeast and mammalian cells. *EMBO J.* **19**, 4577–4588 (2000).
28. Mansell, A. *et al.* Suppressor of cytokine signaling 1 negatively regulates Toll-like receptor signaling by mediating Mal degradation. *Nat. Immunol.* **7**, 148–155 (2006).
29. Cao, X. *et al.* The inositol 3-phosphatase PTEN negatively regulates Fcγ receptor signaling, but supports Toll-like receptor 4 signaling in murine peritoneal macrophages. *J. Immunol.* **172**, 4851–4857 (2004).
30. Gunzl, P. *et al.* Anti-inflammatory properties of the PI3K pathway are mediated by IL-10/DUSP regulation. *J. Leukoc. Biol.* **88**, 1259–1269 (2010).
31. Leslie, N.R., Dixon, M.J., Schenning, M., Gray, A. & Batty, I.H. Distinct inactivation of PI3K signalling by PTEN and 5-phosphatases. *Adv. Enzyme Regul.* **52**, 205–213 (2011).
32. Keck, S., Freudenberg, M. & Huber, M. Activation of murine macrophages via TLR2 and TLR4 is negatively regulated by a Lyn/PI3K module and promoted by SHIP1. *J. Immunol.* **184**, 5809–5818 (2010).
33. Sly, L.M. *et al.* SHIP prevents lipopolysaccharide from triggering an antiviral response in mice. *Blood* **113**, 2945–2954 (2009).
34. Sorimachi, H., Ishiura, S. & Suzuki, K. Structure and physiological function of calpains. *Biochem. J.* **328**, 721–732 (1997).
35. Peltier, J. *et al.* Calpain activation and secretion promote glomerular injury in experimental glomerulonephritis: evidence from calpastatin-transgenic mice. *J. Am. Soc. Nephrol.* **17**, 3415–3423 (2006).
36. Sato, S. *et al.* Toll/IL-1 receptor domain-containing adaptor inducing IFN-β (TRIF) associates with TNF receptor-associated factor 6 and TANK-binding kinase 1, and activates two distinct transcription factors, NF-κB and IFN-regulatory factor-3, in the Toll-like receptor signaling. *J. Immunol.* **171**, 4304–4310 (2003).
37. Doyle, S. *et al.* IRF3 mediates a TLR3/TLR4-specific antiviral gene program. *Immunity* **17**, 251–263 (2002).
38. Chang, E.Y., Guo, B., Doyle, S.E. & Cheng, G. Cutting edge: involvement of the type I IFN production and signaling pathway in lipopolysaccharide-induced IL-10 production. *J. Immunol.* **178**, 6705–6709 (2007).
39. Beutler, B. & Cerami, A. Cachectin, cachexia, and shock. *Annu. Rev. Med.* **39**, 75–83 (1988).
40. Guarda, G. *et al.* Type I interferon inhibits interleukin-1 production and inflammasome activation. *Immunity* **34**, 213–223 (2011).
41. Ohtani, M. *et al.* Mammalian target of rapamycin and glycogen synthase kinase 3 differentially regulate lipopolysaccharide-induced interleukin-12 production in dendritic cells. *Blood* **112**, 635–643 (2008).
42. Androulidaki, A. *et al.* The kinase Akt1 controls macrophage response to lipopolysaccharide by regulating microRNAs. *Immunity* **31**, 220–231 (2009).
43. Laplante, M. & Sabatini, D.M. mTOR signaling in growth control and disease. *Cell* **149**, 274–293 (2012).
44. Cao, W. *et al.* Toll-like receptor-mediated induction of type I interferon in plasmacytoid dendritic cells requires the rapamycin-sensitive PI(3)K-mTOR-p70S6K pathway. *Nat. Immunol.* **9**, 1157–1164 (2008).
45. Guiducci, C. *et al.* PI3K is critical for the nuclear translocation of IRF-7 and type I IFN production by human plasmacytoid predendritic cells in response to TLR activation. *J. Exp. Med.* **205**, 315–322 (2008).
46. Zanoni, I. *et al.* CD14 controls the LPS-induced endocytosis of Toll-like receptor 4. *Cell* **147**, 868–880 (2011).
47. Katakura, K. *et al.* Toll-like receptor 9-induced type I IFN protects mice from experimental colitis. *J. Clin. Invest.* **115**, 695–702 (2005).
48. Zhang, X. *et al.* Type I interferons protect neonates from acute inflammation through interleukin 10-producing B cells. *J. Exp. Med.* **204**, 1107–1118 (2007).
49. Crow, M.K. Type I interferon in organ-targeted autoimmune and inflammatory diseases. *Arthritis Res. Ther.* **12** Suppl 1, S5 (2010).
50. Uno, J.K. *et al.* Altered macrophage function contributes to colitis in mice defective in the phosphoinositide-3 kinase subunit p110δ. *Gastroenterology* **139**, 1642–1653 (2010).
51. Liu, Y. *et al.* A unique feature of Toll/IL-1 receptor domain-containing adaptor protein is partially responsible for lipopolysaccharide insensitivity in zebrafish with a highly conserved function of MyD88. *J. Immunol.* **185**, 3391–3400 (2010).
52. Terebiznik, M.R. *et al.* Elimination of host cell $PtdIns(4,5)P_2$ by bacterial SigD promotes membrane fission during invasion by Salmonella. *Nat. Cell Biol.* **4**, 766–773 (2002).
53. Wang, N. *et al.* A PEST sequence in ABCA1 regulates degradation by calpain protease and stabilization of ABCA1 by apoA-I. *J. Clin. Invest.* **111**, 99–107 (2003).
54. Tompa, P. *et al.* On the sequential determinants of calpain cleavage. *J. Biol. Chem.* **279**, 20775–20785 (2004).

ONLINE METHODS

Mice. Age- and sex-matched mice were used in all experiments. The p110α-, p110β- and p110δ-mutant mice and mice with transgenic expression of calpastatin have been described[11,12,14,35]. All mice were on the C57BL/6 background with the exception of p110β-null and IL-10-deficient mice, which were on the sv/129 and BALB/c background, respectively. All animal experiments were approved by Queen Mary University of London local research ethics committee and were covered by the appropriate licenses (PPL70/7447) under the Home Office Animals Procedures Acts of 1986.

Reagents, antibodies and plasmids. All chemicals, unless stated otherwise, were from Sigma-Aldrich. Source of reagents: recombinant mouse TNF and IL-1β (Peprotech); TLR ligands and LPS *E. coli* (055:B5) (Sigma); ultrapure LPS, *E. coli* (0111:B4), *S. minnesota* (R595) LPS, monophosphoryl lipid A (MPLA) from *S. minnesota*, synthetic MPLA, lipoteichoic acid and Pam_3CSK_4 (tripalmitoyl cysteinyl seryl tetralysine; Invivogen). Antibodies to PI(3)K were as follows: monoclonal anti-110α (for immunoprecipitation; U3A[55]; made in house), rabbit polyclonal anti-110α (for immunoblot analysis; made in-house), a mixture of rabbit antibodies to p110β (for immunoprecipitation; made in-house), rabbit antibody to p110β peptide (for immunoblot analysis; sc-602; Santa Cruz Biotechnologies), anti-p110γ (4252; Cell Signaling Technologies), anti-p110δ (for immunoprecipitation; EPR386; Abcam), anti-p110δ (for immunoblot analysis; sc-7176) and antibody to all p85 (06-195; Upstate). Mouse monoclonal antibody to PtdIns(3,4,5)P_3 (Z-P345b) was from Echelon Biosciences. Antibodies to TLR components were as follows (all from Santa Cruz Biotechnology): anti-TLR4 (sc-293072), anti-MyD88 (sc-74532), anti-TIRAP (for immunoblot analysis; sc-28822) and polyclonal anti-calpain-1 (sc-13390), anti-NF-κB (to p65-RelA; sc-7151) and anti-IRF3 (sc-9082). Antibodies for flow cytometry were as follows (all from BD Pharmingen): fluorescein isothiocyanate–anti-CD8 (53-6.7), allophycocyanin–anti-CD11c (HL3), phycoerythrin–antibody to major histocompatibility complex class II (IA-IE) (M5/114.15.2), fluorescein isothiocyanate–anti-CD40 (323) and fluorescein isothiocyanate–anti–TLR4-MD2 (MTS510). Anti-Akt (9272), antibody to Akt phosphorylated at Thr308 (9275) or Ser473S (9271), antibody to IKKα-IKKβ phosphorylated at Ser176 and Ser180 (2697S), antibody to p38 phosphorylated at Tyr180 and Tyr182 (4531S), anti-GAPDH (2118S) and anti-GST (2624) were all from Cell Signaling Technologies. Sequence encoding 5′ Myc-tagged human p110δ containing the 3′ untranslated region (tagged with the 3′ CaaX sequence, where C is Cys, 'aa' represents alipathic amino acids, and 'X' is any amino acid) was subcloned from the pUAST vector and inserted between the BamHI and XhoI sites of pMX-neo. The plasmids encoding GFP-TIRAP, GST-TIRAP and GST–TIRAP-4x have been described[3]; GST–PLC-δ-PH and GST–Akt-PH were from T. Maffucci; and GST–Hrs-FYVE was provided by H. Stenmark. Flag-tagged TIRAP was from R. Beyaert. Sources of small-molecule inhibitors were as follows: IC87114 and AS604850 (both from Cayman); Dynasore (Sigma); U71123 (Tocris); and TGX-221, PI-103, wortmannin, LY294002, MG-132 and N-ALLN (*N*-acetyl-leucyl-leucyl-norleucinal; all six from Merck4Biosciences).

DC culture and isolation. BMDCs were derived from mouse bone marrow precursors as described[56]. Cells were cultured for 12 d in RPMI-1640 medium (Invitrogen) supplemented with glutamine (Invitrogen), penicillin (Invitrogen), streptomycin (Invitrogen), 2-mercaptoethanol (Sigma) and 10% heat-inactivated FBS (Invitrogen) in the presence of culture supernatants of mouse X63 myeloma cells transfected to express (and used as a source of) mouse granulocyte-macrophage colony-stimulating factor (obtained from D. Gray). The viability and absolute number of BMDCs were assessed by trypan blue exclusion. The DCs obtained were routinely >98% $CD11c^{hi}$ by flow cytometry. Splenic DCs and splenocytes were isolated from mouse spleens by digestion for 30 min at 37 °C with liberase and DNase I (both from Roche). The resulting single-cell suspensions were treated for 2 min at 21 °C with RBC lysis buffer (eBioscience), washed twice with Hank's balanced-salt solution and purified by positive selection with magnetic $CD11c^+$ beads according to the manufacturer's instructions (Miltenyi Biotec).

Flow cytometry of TLR4 intracellular trafficking, endocytosis and phagocytosis. BMDCs and splenic DCs (1×10^5 per condition) were stained with antibodies (identified above) and were analyzed on a CyAn ADP (DakoCyan; BD Coulter). The frequency of up- or downregulation of TLR4 was determined from the median fluorescence intensity (MFI) of receptor expression on stimulated versus unstimulated cells by the following formula: % change = (MFI of stimulated cells at time *t* – MFI of unstimulated cells at time *t*) / MFI of unstimulated cells at time 0) × 100, as reported[57]. For the analysis of phagocytosis and endocytosis, cells were activated for 30 min with LPS (100 ng/ml) before the addition of *E. coli* bioparticles coated with immunoglobulin G (1×10^6 particles per condition), fluorescein isothiocyanate–dextran (10,000 or 40,000 kDa; 100 ng/ml) or fluorescein isothiocyanate–transferrin (20 ng/ml; all from Invitrogen). Subsequently, cells were resuspended in ice-cold PBS containing 5 mM EDTA and 1% BSA, were stained with appropriate antibodies and were analyzed by flow cytometry.

Cell stimulation and generation of NIH3T3 cells stably expressing p110δ with or without or the CAAX domain. The TLR ligands and doses used to activate cells were as follows: LPS from *E. coli* strain O55:B5 or (where indicated) strain O111:B4 (0.0001–1 μg/ml) or MPLA (5 μg/ml) from *S. minnesota*, LPS (100 ng/ml), synthetic MPLA (10 μg/ml), lipoteichoic acid (0.5 μg/ml) or PAM_3SCK_4 (0.5 μg/ml). All inhibitors or vehicle (DMSO (dimethyl sulfoxide)) were added 1 h before cell stimulation. NIH3T3 cells (American Type Culture Collection) and the TIRAP-deficient macrophage cell line[58] were grown in Dulbecco's modified Eagle medium (Invitrogen) supplemented with 10% FBS, 100 units/ml penicillin and 100 mg/ml streptomycin and 7.5 mM HEPES, pH 7.4, at 37 °C in 5% CO_2. NIH3T3 cells were used for the creation of clones stably expressing 5′ Myc-tagged human p110δ with or without the CAAX domain in the pMX vector under a neomycin selection cassette. Cells were selected over 1 month in cell culture medium containing the aminoglycoside G418 sulfate (Invitrogen). Cells were cultured for 2 d in medium without antibiotics before use in experiments.

Calpain activity assay. Calpain assays were done by incubation of recombinant calpain 1 or calpain 2 (1 μg/ml; Sigma) with GST-TIRAP (10 μg/ml) for 30 min at 30 °C in Calpain Assay kit buffer (Merck4Biosciences). Assays were terminated by the addition of 50 mM EDTA to the reaction mixture.

Lipid kinase assay. Lipid kinase activity was tested as described[59] with immunoprecipitates of p85 or p110 made with antibodies for immunoprecipitation (identified above), along with PtdIns(4,5)P_2 and phosphatidylserine (Avanti) in lipid kinase buffer (40 mM Tris-HCl pH 7.4, 200 mM NaCl and 1 mM EGTA) with 100 μM ATP and 10 mM $MgCl_2$.

Lipid-binding assays. PIP strips (Echelon Biosciences) were used for profiling the *in vitro* -binding capacity of recombinant GST-TIRAP. The effect of p110δ kinase activity on the interaction of GST-TIRAP with PtdIns(4,5)P_2 was tested with PI(4,5)P_2-coated 96-well plates (Echelon Biosciences) containing 20 pmol PtdIns(4,5)P_2 per well. Plates were blocked for 1 h at 21 °C with block buffer (10 mM Tris-HCl, pH 8.0, 150 mM NaCl, 0.1% Tween 20 and 0.1% ovalbumin), followed by addition of the GST fusion proteins at varying concentrations (5, 10, 50 or 100 ng/ml) for 30 min at 21 °C. Plates were washed extensively in block buffer, followed by the addition of GST–p110δ-p85 (Jena Bioscience) at the appropriate concentration in lipid kinase buffer (described above), with or without 100 μM ATP, for 30 min at 30 °C. All subsequent washes and incubations were done in lipid kinase buffer. After four washes, anti-GST was added for 1 h at 21 °C, then samples were washed three times and probed for 30 min with horseradish peroxidase–conjugated antibody to mouse immunoglobulin G (RPN4201; GE Healthcare). Plate-bound GST fusion protein was detected at an absorbance of 450 nm with TMB (tetramethyl benzidine) chromogen solution (Invitrogen). The lipids used to create liposomes for vesicle-association assays (Avanti) were prepared as described[6]. Phosphatidylethanolamine-phosphatidylcholine liposomes contained a 3:1 molar ratio of phosphatidylcholine to phosphatidylethanolamine. Liposomes containing phosphatidylinositol species retained that 3:1 ratio but also contained the appropriate amount of PtdIns(4,5)P_2. Recombinant GST–PLC-δ-PH or GST-TIRAP was used at a 'dose' of 50 ng per reaction in the lipid vesicle-association assay.

© 2012 Nature America, Inc. All rights reserved.

Video and confocal microscopy. BMDCs were seeded in 24-well plates on cover glass (VWR Internatiol). After stimulation, cells were fixed for 20 min in ice-cold 4% paraformaldehyde, blocked for 10 min with TBS (25 mM Tris-HCl, pH 7.4, and 150 mM NaCl) and permeabilized for 5 min at 4 °C with TBS containing 50 μM digitonin or 0.2% Triton X-100. Cells were incubated at overnight 4 °C with polyclonal anti-TIRAP (sc-166149; Santa Cruz Biotechnologies), or anti-p65 or anti-IRF3 (antibodies identified above). DAPI (4',6-diamidino-2-phenylindole) was used for staining of nuclei. Staining with recombinant GST–PLC-δ-PH for the detection of PtdIns(4,5)P_2 was done as described[60]. Secondary antibodies conjugated to fluorescein isothiocyanate (mouse, 715-096-150; rabbit, 111-096-144) or indocarbocyanine (mouse, 715-165-151; rabbit, 711-165-152) were from Jackson ImmunoResearch, and Alexa Fluor 647–phalloidin (A22287) was from Invitrogen. For live imaging, BMDCs were transfected with 0.5 μg GFP-TIRAP plasmid through the use of Amaxa Nucleofactor (Lonza). Cells were plated immediately onto 35 mm glass-bottom Petri dishes (MatTek) and were incubated at 37 °C in 5% CO_2. After 18 h, cells were washed and incubated for 1 h in medium without phenol red and then GFP-TIRAP was observed by the acquisition of images of individual cells at intervals of 30 s for up to 60 min in the presence or absence of LPS (100–5,000 ng/ml). Images were exported as TIFF files and movies were assembled and/or analyzed with ImageJ software (http://rsb.info.nih.gov/ij/). Both live and fixed and stained samples were acquired at a thickness of 1 μm with an LSM 710 microscope (Carl Zeiss) equipped with 63× oil-immersion objective with a numerical aperture of 1.3 and a differential interference contrast imaging system. Digital images were processed with Adobe Photoshop CS3 extended (Adobe Systems Inc) or ImageJ software.

Immunoblot analysis, immunoprecipitation and subcellular fractionation. After cell stimulation, cells were washed and lysed for 30 min on ice in the buffer appropriate for the subsequent analysis, immunoblot analysis (radioimmunoprecipitation buffer: 50 mM Tris-HCl, pH 7.5, 1% Nonidet-P40, 0.5% deoxycholic acid, 0.1% SDS, 150 mM NaCl, 10 mM NaF and 1 mM Na_3VO_4); or immunoprecipitation (50 mM HEPES, pH 7.2, 1% NP-40, 5 mM EDTA, 50 mM NaCl, 1 mM Na_3VO_4 and 50 mM NaF), supplemented with protease and phosphatase inhibitors (Roche). Similar amounts of total cell lysate were mixed with Laemmli buffer and separated by 10–12% SDS-PAGE, followed by transfer to nitrocellulose and immunoblot analysis. For subcellular fractionation, cells were washed in PBS and resuspended in hypotonic buffer (20 mM Tris-HCl, pH 7.5, 10 mM $MgCl_2$, 5 mM EDTA, 250 μM sucrose and 200 μM PMSF). Samples were passed five times through a syringe with a 25-gauge needle and were centrifuged at 100,000*g* for 1 h. Supernatants (cytosolic fraction) were transferred to a fresh tube and pellets (membrane fraction) were resuspended in SDS Laemmli sample buffer. Fractions were separated by 12% SDS-PAGE, followed by immunoblot analysis with the appropriate antibodies.

Enzyme-linked immunosorbent assay. Cytokine concentrations in supernatants of BMDCs (5×10^5 cells per ml per condition) or splenocytes (4×10^6 cells per ml) stimulated for 24 h or in serum from mice were measured by enzyme-linked immunosorbent assay kits for mouse TNF, IL-6 or IL-10 (Peprotech) or IL-12p40, IL-12p70 or IFN-β (R&D Systems).

RNA isolation and quantitative RT-PCR. RNA was extracted from mouse spleens with a MagnaPure LC RNA Isolation Kit III (Tissue) (Roche Diagnostics). Reverse-transcription and real-time PCR were done with LightCycler-RNA Master Hyprobes (one-step procedure) on a LightCycler (Roche Diagnostics) for measurement of mRNA for mouse IL-1β, IL10, IFN-β or TNF (primers, **Supplementary Table 2**). The abundance of each specific mRNA was normalized to that of HPRT1 mRNA in the same sample and expressed as relative stimulation.

Protein expression and purification. GST-TIRAP, GST–TIRAP-4x, GST–PLC-δ-PH, GST–Akt-PH and GST–Hrs-FYVE were expressed in the *E. coli* strain BL21 followed by dialysis as described[27].

Statistical analysis. Statistical analysis was done with the nonparametric Mann–Whitney *U* test or, where specified, Student's *t*-test. For three-group comparisons, analysis of variancewas used.

55. Klippel, A., Escobedo, J.A., Hirano, M. & Williams, L.T. The interaction of small domains between the subunits of phosphatidylinositol 3-kinase determines enzyme activity. *Mol. Cell. Biol.* **14**, 2675–2685 (1994).
56. Inaba, K. *et al.* Generation of large numbers of dendritic cells from mouse bone marrow cultures supplemented with granulocyte/macrophage colony-stimulating factor. *J. Exp. Med.* **176**, 1693–1702 (1992).
57. Bachmaier, K. *et al.* E3 ubiquitin ligase Cblb regulates the acute inflammatory response underlying lung injury. *Nat. Med.* **13**, 920–926 (2007).
58. Nagpal, K. *et al.* A TIR domain variant of MyD88 adapter-like (Mal)/TIRAP results in loss of MyD88 binding and reduced TLR2/TLR4 signaling. *J. Biol. Chem.* **284**, 25742–25748 (2009).
59. Foukas, L.C. *et al.* Critical role for the p110α phosphoinositide-3-OH kinase in growth and metabolic regulation. *Nature* **441**, 366–370 (2006).
60. Hammond, G.R., Schiavo, G. & Irvine, R.F. Immunocytochemical techniques reveal multiple, distinct cellular pools of PtdIns4P and PtdIns(4,5)P_2. *Biochem. J.* **422**, 23–35 (2009).

© 2012 Nature America, Inc. All rights reserved.

doi:10.1038/ni.2426

Corrigendum: The p110δ isoform of the kinase PI(3)K controls the subcellular compartmentalization of TLR4 signaling and protects from endotoxic shock

Ezra Aksoy, Salma Taboubi, David Torres, Sandrine Delbauve, Abderrahman Hachani, Maria A Whitehead, Wayne P Pearce, Inma Berenjeno-Martin, Gemma Nock, Alain Filloux, Rudi Beyaert, Veronique Flamand & Bart Vanhaesebroeck
***Nat. Immunol.* 13, 1045–1054 (2012); published online 30 September 2012; corrected after print 8 April 2013**

In the version of this article initially published, the eighth author was identified incorrectly. The correct name is Inma M Berenjeno, and the initials should be I.M.B. in the Author Contributions section. The error has been corrected in the HTML and PDF versions of the article.

© 2012 Nature America, Inc. All rights reserved.